iScience

CellPress
OPEN ACCESS

Article

Synthesize heterogeneous biological knowledge via representation learning for Alzheimer's disease drug repurposing

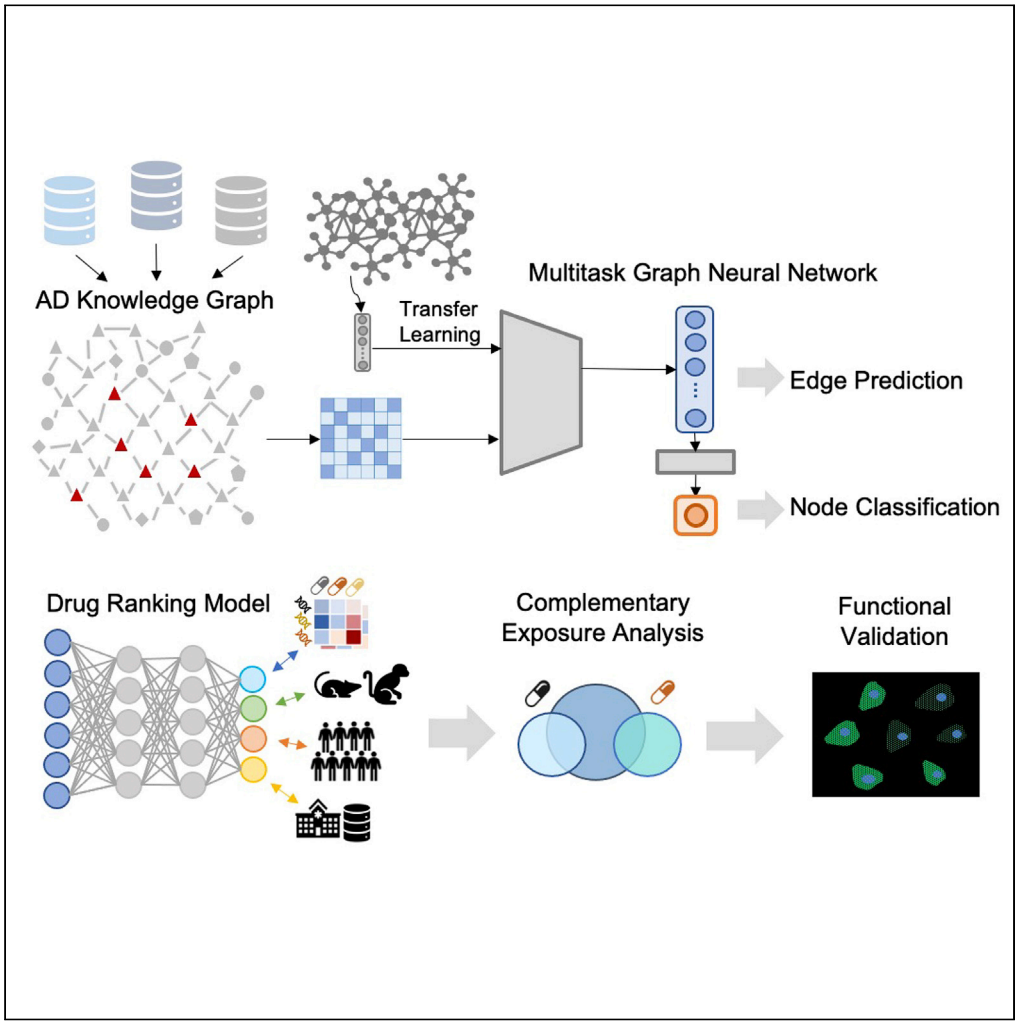

Kang-Lin Hsieh, German Plascencia-Villa, Ko-Hong Lin, George Perry, Xiaoqian Jiang, Yejin Kim

yejin.kim@uth.tmc.edu

Highlights

Our study aims to find AD drugs from biological interactome and structural associations

Our ranking model utilized multi-level drug evidence for drug prioritization

Our predicted drug combinations can reduce Aβ-induced ROS production in neuronal cells

Hsieh et al., iScience 26, 105678
January 20, 2023
https://doi.org/10.1016/j.isci.2022.105678

iScience

CellPress
OPEN ACCESS

Article

Synthesize heterogeneous biological knowledge via representation learning for Alzheimer's disease drug repurposing

Kang-Lin Hsieh,[1,3] German Plascencia-Villa,[2,3] Ko-Hong Lin,[1,3] George Perry,[2] Xiaoqian Jiang,[1] and Yejin Kim[1,4,*]

SUMMARY

Developing drugs for treating Alzheimer's disease has been extremely challenging and costly due to limited knowledge of underlying mechanisms and therapeutic targets. To address the challenge in AD drug development, we developed a multi-task deep learning pipeline that learns biological interactions and AD risk genes, then utilizes multi-level evidence on drug efficacy to identify repurposable drug candidates. Using the embedding derived from the model, we ranked drug candidates based on evidence from post-treatment transcriptomic patterns, efficacy in preclinical models, population-based treatment effects, and clinical trials. We mechanistically validated the top-ranked candidates in neuronal cells, identifying drug combinations with efficacy in reducing oxidative stress and safety in maintaining neuronal viability and morphology. Our neuronal response experiments confirmed several biologically efficacious drug combinations. This pipeline showed that harmonizing heterogeneous and complementary data/knowledge, including human interactome, transcriptome patterns, experimental efficacy, and real-world patient data shed light on the drug development of complex diseases.

INTRODUCTION

Developing drugs for treating Alzheimer's disease (AD) has been extremely challenging and costly. The total cost of developing new AD drugs, including failures, is estimated at $5.7 billion - seven times more than the cost of developing cancer medicines.[1] The most recent FDA approval of Aducanumab is an amyloid beta-directed monoclonal antibody, which aims to treat patients by reducing the buildup of β-amyloid.[2] Despite showing some promising efficacy in removing β-amyloid, only patients with mild stage and amyloid burden can be benefited from the expensive treatment (estimated to cost $56,000 per year).[3] To develop potential treatments in a timely and cost-effective manner, drug repurposing has shown good potential due to the reduced risk of drug toxicity of previously approved drugs. What is even more promising is to study combinatorial drug repositioning, which has demonstrated their potential for synergistically treating complicated diseases, including cancer,[4] diabetes,[5] metabolic syndrome,[6] and cardiovascular disease,[7] thanks to their ability to target multiple pathologies.

Most current AD drug repurposing studies investigate various perspectives, including drug perturbation transcriptome profiles, network pharmacology, and treatment effects in real-world patient data. Transcriptomic-based strategy compares drug-induced gene expression with gene expression in AD specimen,[8–10] which captures integrated molecular changes in different AD pathology. Network pharmacology is another approach that represents a drug's multi-target capacity in a human interaction network.[11–13] This method aims to identify hidden interactions among drugs and proteins (or disease targets) by estimating the proximity between entities in the network. Alternatively, the real-world data approach leverages large sets of patients' drug administration data to obtain off-label indications via treatment effect estimation.[14,15] Each strategy captures different aspects of multimodality and multiscale of the AD treatment landscape. These different approaches provide complementary evidence for potential drugs.[16] Success in a single aspect, however, cannot guarantee clinical effectiveness due to AD's heterogeneous pathogenesis. Consequently, there is a critical need to integrate diverse evidence of transcriptomic observations, heterogeneous biological interactions, preclinical experimental results, and real-world observation to target multiple perspectives in AD drug development.

[1]Center for Secure Artificial Intelligence for Healthcare, School of Biomedical Informatics, University of Texas Health Science Center at Houston, Houston, TX 77030, USA

[2]Department of Neuroscience, Developmental and Regenerative Biology, University of Texas at San Antonio, San Antonio, TX 78729, USA

[3]These authors contributed equally

[4]Lead contact

*Correspondence: yejin.kim@uth.tmc.edu

https://doi.org/10.1016/j.isci.2022.105678

In this study, we proposed an integrated framework for AD drug repurposing. We postulated that by harmonizing drugs' molecular profiles and chemical structures into a knowledge graph, our framework can be used for efficient and systematic identification of potentially repurposable drugs. Here, we implement a graph representation learning model that can simultaneously encapsulate the heterogeneous interactions in the graph and discriminate the molecular determinants of AD into embeddings. Subsequently, our multi-task ranking model integratively prioritizes candidates based on multiple levels of drug evidence, including drug perturbation transcriptome profiles, clinical trial history, drug efficacy in preclinical experiments, and population-based treatment effect estimation. Mechanistic validations showed our candidates' strong efficacy in reducing oxidative stress in mouse brain cell lines. In summary, our key contribution includes:

- Developing advanced deep representation learning to integrate isolated biological knowledge and data, followed by mechanistic validation using mouse brain cells, and
- Covering comprehensive knowledge and data from molecular interactions, transcriptome, preclinical/clinical trials, and population-based treatment effects in real-world patient data.

RESULTS

Alzheimer's disease knowledge graph representation

In this study, we utilized an advanced Graph Neural Network (GNN) approach to identify repurposable drug candidates in the AD knowledge graph. We first integrated biological interactions from multiple human-curated databases to build a comprehensive AD knowledge graph with 30,279 nodes and 398,644 edges. The AD knowledge graph has four types of nodes, including drugs, genes, pathways, and gene ontology (GO), which were connected by seven different interaction types (Figure 1A, Method). We designed a graph autoencoder model to transform the complex relationships within the AD knowledge graph into embedding (Method). Underlying AD etiology is an open research area and current knowledge of AD-related interactions is likely incomplete. A previous study has shown that transfer learning from large pretrained knowledge graph models can enhance model performance in predicting relatively limited domain knowledge such as a COVID-19 biological network.[17] To address the incomplete knowledge of AD, we utilized transfer learning, a machine learning approach that leverages a pretrained model to warm-start the training process and improves performance, from the universal biological database representation in the DRKG network[18] (Method). Additionally, we encouraged gene embedding in the knowledge graph to distinguish high-risk AD-related genes as an auxiliary task (Method). To achieve these goals, we jointly optimized our model to learn the high-risk AD-related genes (node classification) and known relationships (edge classification) among AD knowledge representation.

Evaluate knowledge graph representation

After training the model to learn heterogeneous relationships in the AD knowledge graph, we evaluated how well the embeddings faithfully condense the AD knowledge. Specifically, we investigated whether the embedding could restore the known interactions in the knowledge graph with or without transfer learning (Method, Tables 1 and 2), and visually examined the global position of the node embedding via UMAP plot (Figure 2).[22] As a result, our knowledge graph representation achieved the area under the precision-recall curve (AUPRC) of 0.958 and mean average precision (MAP) of 0.1207 without transfer learning and the AUPRC of 0.988 and the MAP of 0.3195 with transfer learning, which are higher than universal embedding (Method) that achieved the AUPRC of 0.648 and MAP of 0.1013 (Table 1). To detect any under-representation in the embeddings, we separately evaluated the accuracy of each edge type. Our model consistently predicted most edge types. The Drug-GO interactions are relatively harder to predict, whereas gene-gene interactions are easier to predict (Table 2). By ablating one edge type and measuring the edge prediction accuracy, we found that the drug-target or drug-pathway interactions are the most unique interactions that are hard to be inferred if they are excluded (Table S1). For the AD-related gene prediction task, the gene embedding was well-trained to distinguish the 743 AD-related genes from other remaining genes with an area under the receiver operating curve (AUROC) of 0.947 and AUPRC of 0.583 (Table S2). Analysis showed that the model incorrectly predicted TRIOBP (probability = 0.0476) as a non-AD gene, likely due to the connection to fewer neighboring nodes and thus limited the model propagation, compared with ADAM10 (probability = 0.826) (Figure S1).

Visualizing the embedding via UMAP, we found that the overall node distribution is generally dispersed throughout the plot rather than clustered with the same node type (Figure 2). Undergoing clinical trial

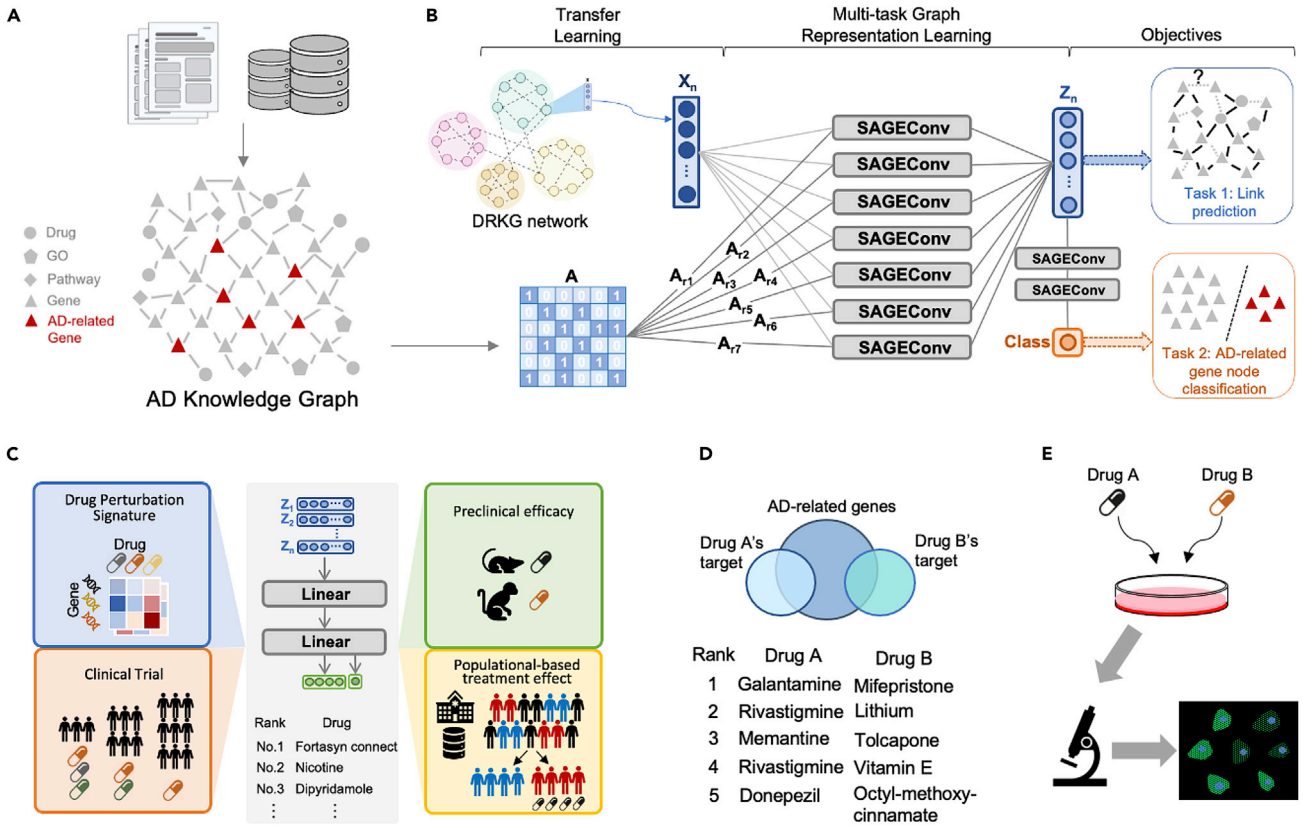

Figure 1. Study workflow

(A) Build the AD knowledge graph with nodes (drugs, genes, pathways, and gene ontology) and edges (drug-target interaction, drug-drug structural similarity, gene-gene interaction, gene-pathway association, gene-GO association, and drug-GO association).

(B) Derive the node embeddings using our multi-relational variational graph autoencoder.[19,20]

(C) Multi-task ranking model was used to rank drug candidates based on multi-level evidence in drug perturbation signatures, preclinical efficacies, clinical trials, and population-based treatment effects.

(D) Search drug combinations satisfying complementary exposure patterns[21] using the high-ranked drug candidates.

(E) Validate drug combinations using oxidative stress assays on HT22 Mouse Hippocampal Neuronal Cell Line.

drugs are aggregated into three main groups, each with similar therapeutic or pharmacological categories, implying the node embedding well reflects the contextual information (Figure 2). In all, the high accuracy in masked interaction prediction and AD-related gene prediction, together with global distribution in UMAP plot, implies that the node embedding faithfully captures the local and global network topology of the AD knowledge graph regardless of edge types, with the help of universal embedding that provides complementary information to restore the masked AD knowledge. This implied the potential applicability of our derived embeddings for drug repurposing tasks.

Identifying drug candidates using multi-level evidence

Most prior studies have identified repurposable drugs based on missing edge prediction between drug and target in GNN.[23,24] However, this approach is heavily dependent on the reliability of AD-related high-risk genes, which is still an open research question. Instead, our approach is a "reverse engineering" approach that utilizes drugs with non-trivial evidence in preclinical/clinical stages and identifies similar drugs in terms of AD biology. After synthesizing the heterogeneous AD knowledge into the embedding, we prioritize repurposable drugs by taking four categories of evidence as labels, including transcriptomic reversed patterns, mechanistic efficacies, population-based treatment effects (Table S3), and clinical trials (Method). Our multi-task ranking model utilizes a pairwise ranking loss to prioritize repurposable drugs (Method). As a result, the ranking model accuracy was AUROC = 0.910 and AUPRC = 0.472 to predict drugs with at least one of the drug efficacies labels. We presented the top-ranked drugs in Table S4 (precision at top 600 = 0.42) and highlighted the top 10 in Table 3.

Table 1. Overall edge prediction accuracy using AD knowledge graph's node embedding

	Pretrained universal embedding	AD knowledge graph representation without transfer learning	AD knowledge graph representation with transfer learning
AUROC	0.565	0.959	0.991
AUPRC	0.648	0.958	0.988
Mean reciprocal rank (MRR)	0.0057	0.0264	0.1112
Mean average precision (MAP)	0.1013	0.1207	0.3195
Precision@10	0.1235	0.0613	0.2517

Edge prediction performance of each set of embeddings.

Identifying drug combination using complementary exposure pattern analysis

As indicated by the complexity of the AD knowledge graph, using single drugs to treat AD might result in limited effects. To improve treatment efficacy, we identified potential drug combinations from the top-ranked drugs (Table S4) and existing FDA-approved AD drugs. Four conventional drugs treat symptoms in AD – rivastigmine, galantamine, donepezil, and memantine, are generally effective in two main mechanisms of action, cholinesterase (AChE) inhibitors or *N*-methyl D-aspartate (NMDA) antagonists. These drugs are intended to maintain or stabilize neuronal function, management of behavioral symptoms, and slow down the rate of memory loss by regulating neurotransmitters. In general, AChE inhibitors are recommended for the treatment of mild-to-moderate AD, whereas NMDA antagonist is prescribed to treat moderate-to-severe AD.[36] Unfortunately, after high-dose exposures to these drugs, patients often experience various CNS and metabolic side effects, including nausea, loss of appetite, weight loss, headache, and confusion, and so forth. To maximize the effect while attempting to minimize adverse reactions by reducing dosage of the conventional medications, we proposed to discover alternative treatments for AD by combining the FDA-approved AD drugs with the top-ranked drugs identified in our computational model.

To identify drug combinations with synergistic interactions without degradation in safety, we leveraged the "Complementary Exposure Pattern" (Method) analysis, which has been successfully applied to drug repurposing in hypertension[37] and COVID-19.[17] The theory indicates that a drug combination is therapeutically effective if the targets of the drugs hit the disease module without overlap.[37] Table 4 summarized the identified drug combinations in our top 30 drugs and the number of their common targets. A total of 10

Table 2. Edge prediction accuracy of each edge type

Edge type to predict	Pretrained universal embedding		AD knowledge graph representation without transfer learning		AD knowledge graph representation with transfer learning	
	AUROC	AUPRC	AUROC	AUPRC	AUROC	AUPRC
Drug - gene	0.528	0.489	0.863	0.795	0.960	0.941
Gene - gene	0.987	0.985	0.936	0.887	0.991	0.984
Drug - GO	0.604	0.554	0.657	0.578	0.889	0.895
Gene - GO	0.613	0.593	0.925	0.912	0.985	0.974
Drug - pathway	0.282	0.376	0.989	0.988	0.998	0.995
Drug - drug structural similarity	0.897	0.867	0.981	0.985	0.994	0.990
Gene - pathway	0.397	0.459	0.590	0.639	0.956	0.947

To examine how well each edge type is preserved in the node embedding, we measured the edge prediction accuracy for each edge type separately. The accuracy values for all edge types were consistent without any edge types being under-fitted. For AD knowledge graph representation without transfer learning, we initialized the node embedding with random initialization.

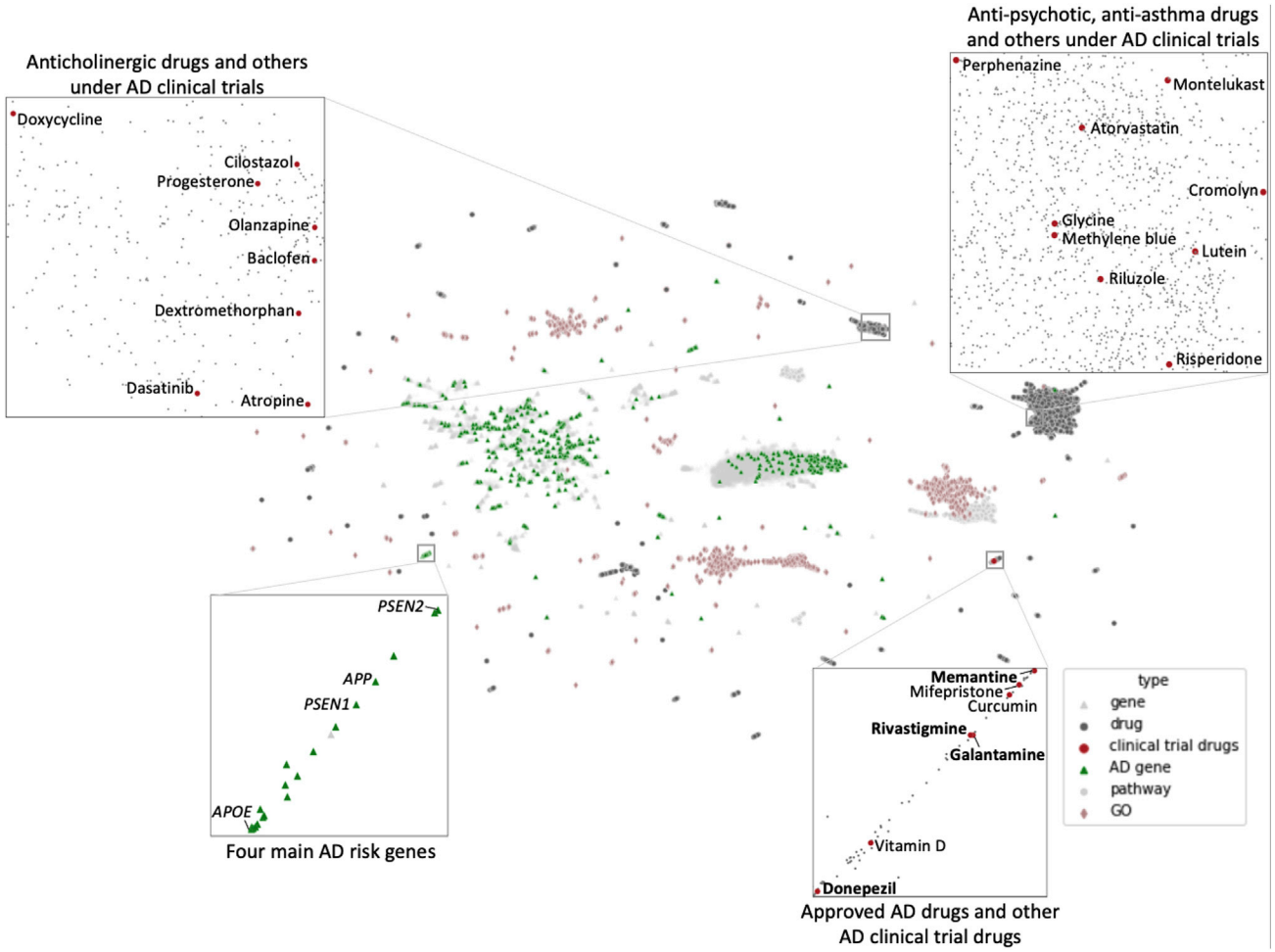

Figure 2. UMAP plot for the lower-dimensional projection of node embedding

Nodes with similar embeddings are adjacent in the UMAP plot. Four current FDA-approved AD drugs were indicated in bold text. Four main AD risk genes (green triangle) and undergoing clinical trial drug (red circle) clusters were highlighted in subplots. Genes, which are in gray triangles, were mixed with drugs, which are in the black rounds. Gene ontologies (pink diamond) and pathways (light gray circle) are adjacent to genes and drugs.

combinations satisfied the criteria, where the combination of Galantamine and Mifepristone has the widest coverage to the AD module. The efficacies of these combinations were further validated using neural cell models.

In vitro validation on safety, tolerability, and neuronal responses of drug combinations

To examine the potential efficacies of our predicted drug combinations, we mechanistically validated the top-ranked drug combinations by measuring cytotoxicity and oxidative stress on hippocampal neurons (Method, Figure 1F). Our results suggest significant efficacy in reducing reactive oxygen species (ROS) levels by multiple drug combinations, implying the potential applications of combining existing and novel drug candidates for AD.

Memantine functions as an antagonist of glutamatergic NMDA receptors, type 3 serotonin (5HT3) receptor, and nicotinic acetylcholine receptor (nAChRs), allowing neuronal availability of neurotransmitters and improving cognition and behavior in patients with moderate-to-severe AD. In combination with Tolcapone, an FDA-approved catechol-*O*-methyltransferase inhibitor used in the management of Parkinson disease to increase levels of peripheral dopamine, we observed safety and tolerability in cholinergic neurons during the dose- and time-course treatments. The combination can reduce the production of ROS by 5.6 $\pm$ 2.2%. In the presence of Aβ, Mem + Tolca was able to reestablish oxidative stress to basal levels, whereas the

Table 3. Selected promising drugs with supporting evidence and literature

Name	Pharmacological classes	Primary indications	Main targets	Multi-level evidence				Reference
				Clinical trials	Transcriptomic relevance	Population-based treatment effect	Preclinical trial	
Galantamine	Acetylcholinesterase inhibitor	Mild to moderate AD	ACHE, CHRNA7, BCHE	+	+		+	Rockwood et al.[25]
Melatonin	Acetamides	Insomnia	MTNR1A, MTNR1B, ESR1	+	+		+	Menczel Schrire et al.[26]
Celecoxib	NSAID	Osteoarthritis, Rheumatoid arthritis	PTGS2, PDPK1, CDH11	+	+		+	Mhillaj et al.[27]
Mifepristone	Hormone modulators	Early pregnancy termination	PGR, NR3C1, KLK3	+				Pomara et al.[28]
Trazodone	Antidepressants	Major depressive disorder	HTR2A, HTR2C, SLC6A4	+		+		Ashford[29]
Ibuprofen	NSAID	Pain, Osteoarthritis, Rheumatoid arthritis	COX-1, COX-2, PTGS2	+		+	+	Van Dam[30]
Avagacestat (BMS-708163)	Anti-amyloid	NA	γ-secretase	+				Tong et al.[31]; Hopkins[32]
Rosiglitazone	Thiazolidinedione	Type 2 diabetes	PPARG, ACSL4, PPARA	+	+		+	Escribano et al.[33]
Amphotericin B	Anti-infectives	Fungal infections	Ergosterol					Hartsel and Weiland[34]
Physostigmine	Anticholinergic	Glaucoma	ACHE, CHRNA4, CHRNB2				+	Winblad et al.[35]

+: positive evidence, blank: not investigated.

single Mem treatment presented a 5.5 ± 2.7% increase (Figure 3). Memantine is usually administered in combination with Donepezil, but in combination with Tolcapone, the drugs could have significant benefits on global and functional outcomes in AD subjects.[38,39]

Donepezil, an AChE inhibitor that allows an increase in acetylcholine in cholinergic neurons, has been used for 25 years to delay cognitive decline and symptoms of AD. Among our top-ranked drugs, the combination of Don + Octyl-methoxycinnamate showed high tolerability and safety. Functionally, Donepezil effectively reduced the amount of ROS by 6.82–7.98%, but its combination with Octyl-met showed a slight increase by

Table 4. Drug combinations that satisfy the complementary exposure pattern from the top 30 drugs

Drug A	Drug B	# AD target A hits	# AD target B hits	# AD target A or B hit
Galantamine	Mifepristone	7	90	97
Rivastigmine	Lithium	7	59	66
Memantine	Tolcapone	10	28	38
Rivastigmine	Vitamin E	7	29	36
Donepezil	Octyl-methoxycinnamate	25	8	33
Galantamine	Diclofenac	7	26	33
Rivastigmine	Diclofenac	7	26	33
Galantamine	Caffeine	7	25	32
Donepezil	Manidipine	25	6	31
Memantine	Octy-lmethoxycinnamate	10	8	18

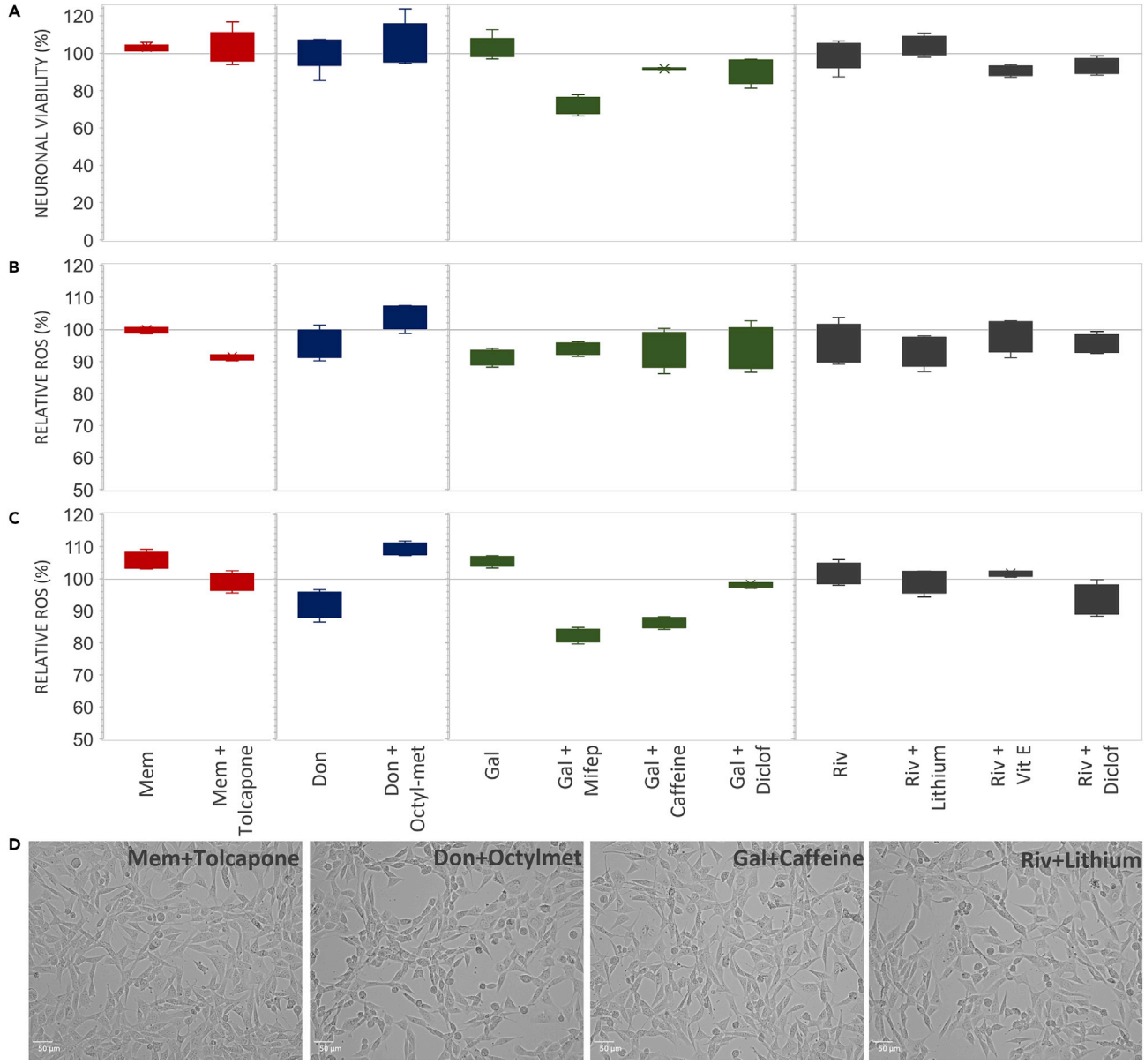

Figure 3. Neuronal responses to drug combinations

(A) Neuronal viability after 24 h with 50 μM of drug combinations.

(B) Quantification of intracellular oxidative stress (DCFDA fluorescence) after 24 h with 50μM of drug A + 50μM of drug B.

(C) Quantification of intracellular oxidative stress (DCFDA fluorescence) of neurons dosed with 10 μM Aβ, after 24 h with 50μM of drug A + 50μM of drug B. All datasets were normalized to neurons dosed with vehicle (DMSO) and the control was represented as a horizontal line at 100% across all the treatments. Each treatment was performed in triplicates.

(D) Live-cell bright-field imaging of neurons dosed for 24 h with 50μM of drug A + 50μM of drug B.

4.3–9.1% (Figure 3), this could be related to the limited solubility of this active compound and that it is usually employed in topical formations.

Galantamine is a weak AChE inhibitor and allosteric potentiator of acetylcholine receptors, intended to treat the progression of symptoms, memory loss, and thinking ability in mild-to-moderate AD. Gal prevents acetylcholine processing and stimulation of its release by nicotinic receptors. Our results showed that combining Galantamine with Mifepristone, Caffeine, or Diclofenac, can lead to a reduction in oxidative stress responses by 5.8–6.3%. These neuroprotective effects were more evident in the neurons dosed

with Aβ, decreasing ROS production at 17.7% in Gal + Mifep, 13.5% in Gal + Caffeine, and 2% in Gal + Diclofenac, whereas single Galantamine treatment presented a 5.5% increase in neuronal oxidative stress (Figure 3). Previous studies found that the neuroprotective effect of Mifepristone is related to preventing stress-induced responses, protecting neurons from undergoing programmed cell death (apoptosis), and increasing AMPA receptor expression,[40] while Mifepristone may also promote rapid repair of the synaptic alterations in the hippocampus.[41] Alternatively, Caffeine can activate noradrenaline neurons and the release of dopamine, counteracting the development of cognitive impairment as an antioxidant.[42] On the other hand, Diclofenac, an anti-inflammatory drug targeting voltage-dependent K^+ channels, also has neuroprotective effects in neurons and showed favorable outcomes of reducing the AD risk in veterans.[43,44]

Acting as an AChE and butyrylcholinesterase inhibitor, Rivastigmine is used to treat memory loss and improve thinking abilities in patients with AD. The tolerability and safety of Rivastigmine alone or in combination with Lithium, Vitamin E, and Diclofenac showed well tolerance in cholinergic neurons (Figure 3). Neuronal responses indicated that these active compounds can effectively reduce oxidative stress in neurons by 4.8–6.2%. In the presence of Aβ, Rivastigmine, Riv + Lithium, and Riv + Vit E showed similar levels of ROS reduction, whereas Riv + Diclof can further reduce 6.8% of intracellular ROS (Figure 3). Lithium, currently under Phase III clinical trials for treating AD, can reduce excitatory neurotransmitters and increase GABA, and prevent cognitive and functional impairment in mild dementia.[45,46] Vitamin E (tocopherol), a neuroprotectant with antioxidant properties, is under clinical trials (Phase II/III) to determine its effects on clinical progression of AD.[47] Taken together, this study successfully identified several drug candidates with high potential of treating AD and have optimistic therapeutic values, and numerous drug combinations suggested by our pipeline also showed promising efficacies in reducing oxidative stress in neural cell models.

DISCUSSION

The objective of this study was to provide proof-of-concept hypotheses on drug combinations to treat AD, utilizing knowledge graph embedding of heterogeneous interactome and multi-task learning of complementary evidence on drug efficacies. Our AD knowledge graph embedding boosted by pretrained universal pharmacological embedding integrates not only the human interactomes but also millions of interactions in public biomedical literature. Our multi-task learning of AD-related genes and multi-level drug efficacy aims to close the gap between the scattered knowledge in AD research.

Our methodology tackles important challenges to harmonize fragmented multimodal data. Recently, several prior works have used the graph neural network approach for drug development, either for general purpose,[23,48] for rare diseases,[49] or for specific diseases including COVID-19[17,18,50] and AD.[51] Our methodological strength over the prior approach includes (1) transfer learning of universal embedding to integrate broader modality to address the incomplete knowledge, (2) multi-task learning for multimodal interactions, AD-related genes, and multi-level drug efficacy to mitigate the lack of established therapeutic targets, and (3) *in vitro* validation of the computational model via hippocampal neuron cells.

Drug combinations that we validated are less toxic (FDA-approved drugs) and economically viable (generic drugs). AD is multifactorial and the use of multi-target therapeutic interventions addressing several molecular targets seems to be an alternative approach to modify the course of AD progression.[52] Different clinical studies demonstrate that combination therapy is more efficient than monotherapy, especially in mild-to-moderate AD to slow down the rate of cognitive impairment. Our integrative approach has identified promising drug combinations adjuvant to existing FDA-approved AD drugs. All drug combinations we identified are available in generic formulations, making them economically viable and available as an alternative to patented formulations with a high monthly cost (>500 USD).

Limitations of the study

Our study has several limitations. Instead of a mechanism-based approach that identifies therapeutic targets first and identifies drugs interacting with them, our approach relies on historical or data-driven evidence, such as estimated drug efficacy (transcriptomic reversed patterns, population-based treatment effect) and established efficacy (preclinical or clinical trials). If this data-driven drug efficacy is biased, our model's drug ranking can be also biased. For example, drugs targeting amyloid beta are much more studied than drugs targeting other pathologies, thus our model has a potential risk to trap in the circularity of

failed drugs targeting amyloid beta. Population-based treatment effects in real-world data can partly mitigate the bias in historical research data toward amyloid-beta. Finally, *in vitro* patterns do not guarantee *in vivo* efficacy or treatment outcomes in patients due to various reasons, including diverse genomics profiles in AD transgenic mouse models, variation of PK/PD, bioavailability in the human body, and so forth. However, our contribution is to efficiently and comprehensively refine a list of candidates from a huge set of compounds, accelerating the costly early-stage drug screening step in the drug development process. Our computational predictions and *in vitro* validations provided a list of highly promising drug combinations and opened future research opportunities.

Despite the limitations, our drug repurposing strategy has a broad impact not only on AD but also on complex diseases, in which complex mechanisms of action and therapeutic targets are open questions. The well-known deficiency of knowledge and insufficiency of data in AD research, when studied separately, prevent us from capturing the complex AD's heterogeneous pathogenesis. Our pipeline integrates complementary information at multiple stages (such as transcriptomic patterns, preclinical efficacy, clinical partial effectiveness, and population-based treatment effect) to better identify promising drug combinations. Hypotheses generated from this integrative approach may shed light on complex disease drug development.

STAR★METHODS

Detailed methods are provided in the online version of this paper and include the following:

- KEY RESOURCES TABLE
- RESOURCE AVAILABILITY
  - Lead contact
  - Materials availability
  - Data and code availability
- METHOD DETAILS
  - Build Alzheimer's disease knowledge graph
  - Knowledge graph representation
  - Transfer learning from a comprehensive drug knowledge graph
  - Node classification to differentiate AD-related genes in the knowledge graph
  - Validating the quality of knowledge graph representation
  - Identification of multi-level evidence for drug efficacy
  - Prioritizing repurposable drugs with multiple evidence
  - Drug combination identification
  - *In vitro* validation on safety, tolerability, drug combinations
- QUANTIFICATION AND STATISTICAL ANALYSIS

SUPPLEMENTAL INFORMATION

Supplemental information can be found online at https://doi.org/10.1016/j.isci.2022.105678.

ACKNOWLEDGMENTS

KH was supported by CPRIT RP140113 (Computational Cancer Biology Training Program Fellowship from Gulf Coast Consortia). XJ is CPRIT Scholar in Cancer Research (RR180012), and he was supported in part by the Christopher Sarofim Family Professorship, UT Stars award, UTHealth startup, the National Institute of Health (NIH) under award number R01AG066749. YK was supported in part by UTHealth startup and the National Institute of Health (NIH) under award number R01AG066749.

AUTHOR CONTRIBUTIONS

XJ and YK provided motivation for the study and contributed to the idea development; KH, KL, and YK developed the computational method; KH and KL performed computational experiments;

GPV and GP performed biological experiments; KH, KL, and YK wrote the initial article; KH, GPV, KL, GP, XJ, and YK edited the article. All authors have read and approved the final article.

DECLARATION OF INTERESTS

The authors have no conflict of interest to declare.

Received: July 15, 2022
Revised: November 4, 2022
Accepted: November 23, 2022
Published: January 20, 2023

REFERENCES

1. Cummings, J., Reiber, C., and Kumar, P. (2018). The price of progress: funding and financing Alzheimer's disease drug development. Alzheimers Dement. *4*, 330–343.

2. Office of the Commissioner (2021). FDA grants accelerated approval for Alzheimer's drug. https://www.fda.gov/news-events/press-announcements/fda-grants-accelerated-approval-alzheimers-drug.

3. Fleming, W.K., Brown, C.R., and Shrank, W.H. (2020). Costly new alzheimer disease medications on the horizon—financing alternatives for medicare. JAMA Health Forum *1*, e201148. https://doi.org/10.1001/jamahealthforum.2020.1148.

4. Kim, Y., Zheng, S., Tang, J., Jim Zheng, W., Li, Z., and Jiang, X. (2021). Anticancer drug synergy prediction in understudied tissues using transfer learning. J. Am. Med. Inform. Assoc. *28*, 42–51.

5. Cahn, A., and Cefalu, W.T. (2016). Clinical considerations for use of initial combination therapy in type 2 diabetes. Diabetes Care *39*, S137–S145.

6. Bakris, G., Molitch, M., Hewkin, A., Kipnes, M., Sarafidis, P., Fakouhi, K., Bacher, P., and Sowers, J.; STAR Investigators (2006). Differences in glucose tolerance between fixed-dose antihypertensive drug combinations in people with metabolic syndrome. Diabetes Care *29*, 2592–2597. https://doi.org/10.2337/dc06-1373.

7. Working Group on the Summit on Combination Therapy for CVD, Yusuf, S., Attaran, A., Bosch, J., Joseph, P., Lonn, E., McCready, T., Mente, A., Nieuwlaat, R., Pais, P., et al. (2014). Combination pharmacotherapy to prevent cardiovascular disease: present status and challenges. Eur. Heart J. *35*, 353–364.

8. Siavelis, J.C., Bourdakou, M.M., Athanasiadis, E.I., Spyrou, G.M., and Nikita, K.S. (2016). Bioinformatics methods in drug repurposing for Alzheimer's disease. Brief. Bioinform. *17*, 322–335. https://doi.org/10.1093/bib/bbv048.

9. Williams, G., Gatt, A., Clarke, E., Corcoran, J., Doherty, P., Chambers, D., and Ballard, C. (2019). Drug repurposing for Alzheimer's disease based on transcriptional profiling of human iPSC-derived cortical neurons. Transl. Psychiatry *9*, 220.

10. Sirota, M., Dudley, J.T., Kim, J., Chiang, A.P., Morgan, A.A., Sweet-Cordero, A., Sage, J., and Butte, A.J. (2011). Discovery and preclinical validation of drug indications using compendia of public gene expression data. Sci. Transl. Med. *3*, 96ra77.

11. Pham, T.-H., Qiu, Y., Zeng, J., Xie, L., and Zhang, P. (2020). A deep learning framework for high-throughput mechanism-driven phenotype compound screening. bioRxiv. 2020.07.19.211235. https://doi.org/10.1101/2020.07.19.211235.

12. Huang, L., Brunell, D., Stephan, C., Mancuso, J., Yu, X., He, B., Thompson, T.C., Zinner, R., Kim, J., Davies, P., and Wong, S.T.C. (2019). Driver network as a biomarker: systematic integration and network modeling of multi-omics data to derive driver signaling pathways for drug combination prediction. Bioinformatics *35*, 3709–3717.

13. Chen, Y., and Xu, R. (2019). Context-sensitive network analysis identifies food metabolites associated with Alzheimer's disease: an exploratory study. BMC Med. Genom. *12*, 17. https://doi.org/10.1186/s12920-018-0459-2.

14. Geifman, N., Brinton, R.D., Kennedy, R.E., Schneider, L.S., and Butte, A.J. (2017). Evidence for benefit of statins to modify cognitive decline and risk in Alzheimer's disease. Alzheimer's Res. Ther. *9*, 10. https://doi.org/10.1186/s13195-017-0237-y.

15. Zissimopoulos, J.M., Barthold, D., Brinton, R.D., and Joyce, G. (2017). Sex and race differences in the association between statin use and the incidence of alzheimer disease. JAMA Neurol. *74*, 225–232.

16. Cheng, F., Desai, R.J., Handy, D.E., Wang, R., Schneeweiss, S., Barabási, A.L., and Loscalzo, J. (2018). Network-based approach to prediction and population-based validation of in silico drug repurposing. Nat. Commun. *9*, 2691.

17. Hsieh, K., Wang, Y., Chen, L., Zhao, Z., Savitz, S., Jiang, X., Tang, J., and Kim, Y. (2021). Drug repurposing for COVID-19 using graph neural network and harmonizing multiple evidence. Sci. Rep. *11*, 23179.

18. Zeng, X., Song, X., Ma, T., Pan, X., Zhou, Y., Hou, Y., Zhang, Z., Karypis, G., and Cheng, F. (2020). Repurpose Open Data to Discover Therapeutics for COVID-19 Using Deep Learning.

19. Kipf, T.N., and Welling, M. (2016). Variational Graph Auto-Encoders.

20. Schlichtkrull, M., Kipf, T.N., Bloem, P., van den Berg, R., Titov, I., and Welling, M. (2017). Modeling Relational Data with Graph Convolutional Networks.

21. Zhou, Y., Hou, Y., Shen, J., Huang, Y., Martin, W., and Cheng, F. (2020). Network-based drug repurposing for novel coronavirus 2019-nCoV/SARS-CoV-2. Cell Discov. *6*, 14–18.

22. McInnes, L., Healy, J., and Melville, J. (2018). UMAP: Uniform Manifold Approximation and Projection for Dimension Reduction.

23. Mohamed, S.K., Nováček, V., and Nounu, A. (2020). Discovering protein drug targets using knowledge graph embeddings. Bioinformatics *36*, 603–610.

24. Zitnik, M., Agrawal, M., and Leskovec, J. (2018). Modeling polypharmacy side effects with graph convolutional networks. Bioinformatics *34*, i457–i466.

25. Rockwood, K., Mintzer, J., Truyen, L., Wessel, T., and Wilkinson, D. (2001). Effects of a flexible galantamine dose in Alzheimer's disease: a randomised, controlled trial. J. Neurol. Neurosurg. Psychiatry *71*, 589–595.

26. Menczel Schrire, Z., Phillips, C.L., Duffy, S.L., Marshall, N.S., Mowszowski, L., La Monica, H.M., Gordon, C.J., Chapman, J.L., Saini, B., Lewis, S.J.G., et al. (2021). Feasibility of 3-month melatonin supplementation for brain oxidative stress and sleep in mild cognitive impairment: protocol for a randomised, placebo-controlled study. BMJ Open *11*, e041500.

27. Mhillaj, E., Papi, M., Paciello, F., Silvestrini, A., Rolesi, R., Palmieri, V., Perini, G., Fetoni, A.R., Trabace, L., and Mancuso, C. (2020). Celecoxib exerts neuroprotective effects in β-amyloid-treated SH-SY5Y cells through the regulation of heme oxygenase-1: novel insights for an old drug. Front. Cell Dev. Biol. *8*, 561179.

28. Pomara, N., Doraiswamy, P.M., Tun, H., and Ferris, S. (2002). Mifepristone (RU 486) for Alzheimer's disease. Neurology *58*, 1436.

29. Ashford, J.W. (2019). Treatment of Alzheimer's disease: trazodone, sleep, serotonin, norepinephrine, and future directions. J. Alzheimers Dis. *67*, 923–930.

30. Van Dam, D., Coen, K., and De Deyn, P.P. (2010). Ibuprofen modifies cognitive disease progression in an Alzheimer's mouse model. J. Psychopharmacol. *24*, 383–388.

31. Tong, G., Castaneda, L., Wang, J.-S., Sverdlov, O., Huang, S.-P., Slemmon, R., Gu, H., Wong, O., Li, H., Berman, R.M., et al. (2012). Effects of single doses of avagacestat (BMS-708163) on cerebrospinal fluid Aβ levels in healthy young men. Clin. Drug Investig. *32*, 761–769.

32. Hopkins, C.R. (2012). ACS chemical neuroscience molecule spotlight on BMS-708163. ACS Chem. Neurosci. *3*, 149–150.

33. Escribano, L., Simón, A.M., Pérez-Mediavilla, A., Salazar-Colocho, P., Río, J.D., and Frechilla, D. (2009). Rosiglitazone reverses memory decline and hippocampal

glucocorticoid receptor down-regulation in an Alzheimer's disease mouse model. Biochem. Biophys. Res. Commun. *379*, 406–410.

34. Hartsel, S.C., and Weiland, T.R. (2003). Amphotericin B binds to amyloid fibrils and delays their formation: a therapeutic mechanism? Biochemistry *42*, 6228–6233.

35. Winblad, B., Giacobini, E., Frölich, L., Friedhoff, L.T., Bruinsma, G., Becker, R.E., and Greig, N.H. (2010). Phenserine efficacy in Alzheimer's disease. J. Alzheimers Dis. *22*, 1201–1208.

36. Plascencia-Villa, G., and Perry, G. (2022). Alzheimer's disease pharmacology. Ref. Modul. Biomed. Sci. 34–63. https://doi.org/10.1016/b978-0-12-820472-6.00018-9.

37. Cheng, F., Kovács, I.A., and Barabási, A.L. (2019). Network-based prediction of drug combinations. Nat. Commun. *10*, 1197.

38. Fremont, R., Manoochehri, M., Armstrong, N.M., Mattay, V.S., Apud, J.A., Tierney, M.C., Devanand, D.P., Gazes, Y., Habeck, C., Wassermann, E.M., et al. (2020). Tolcapone treatment for cognitive and behavioral symptoms in behavioral variant frontotemporal dementia: a placebo-controlled crossover study. J. Alzheimers Dis. *75*, 1391–1403.

39. Apud, J.A., Mattay, V., Chen, J., Kolachana, B.S., Callicott, J.H., Rasetti, R., Alce, G., Iudicello, J.E., Akbar, N., Egan, M.F., et al. (2007). Tolcapone improves cognition and cortical information processing in normal human subjects. Neuropsychopharmacology *32*, 1011–1020.

40. Ghoumari, A.M., Piochon, C., Tomkiewicz, C., Eychenne, B., Levenes, C., Dusart, I., Schumacher, M., and Baulieu, E.E. (2006). Neuroprotective effect of mifepristone involves neuron depolarization. FASEB J *20*, 1377–1386.

41. Wu, L.-M., Han, H., Wang, Q.-N., Hou, H.-L., Tong, H., Yan, X.-B., and Zhou, J.-N. (2007). Mifepristone repairs region-dependent alteration of synapsin I in hippocampus in rat model of depression. Neuropsychopharmacology *32*, 2500–2510.

42. Londzin, P., Zamora, M., Kąkol, B., Taborek, A., and Folwarczna, J. (2021). Potential of caffeine in Alzheimer's disease—a review of experimental studies. Nutrients *13*, 537. https://doi.org/10.3390/nu13020537.

43. Stuve, O., Weideman, R.A., McMahan, D.M., Jacob, D.A., and Little, B.B. (2020). Diclofenac reduces the risk of Alzheimer's disease: a pilot analysis of NSAIDs in two US veteran populations. Ther. Adv. Neurol. Disord. *13*. 1756286420935676. https://doi.org/10.1177/1756286420935676.

44. Naeem, S., Najam, R., Khan, S.S., Mirza, T., and Sikandar, B. (2019). Neuroprotective effect of diclofenac on chlorpromazine induced catalepsy in rats. Metab. Brain Dis. *34*, 1191–1199.

45. Forlenza, O.V., Radanovic, M., Talib, L.L., and Gattaz, W.F. (2019). Clinical and biological effects of long-term lithium treatment in older adults with amnestic mild cognitive impairment: randomised clinical trial. Br. J. Psychiatry *215*, 668–674.

46. Malhi, G.S., Tanious, M., Das, P., Coulston, C.M., and Berk, M. (2013). Potential mechanisms of action of lithium in bipolar disorder. Current understanding. CNS Drugs *27*, 135–153.

47. Sen, C.K., Khanna, S., and Roy, S. (2004). Tocotrienol: the natural vitamin E to defend the nervous system? Ann. N. Y. Acad. Sci. *1031*, 127–142.

48. gnn4dr gnn4dr/DRKG. GitHub. https://github.com/gnn4dr/DRKG.

49. Sosa, D.N., Derry, A., Guo, M., Wei, E., Brinton, C., and Altman, R.B. (2020). A literature-based knowledge graph embedding method for identifying drug repurposing opportunities in rare diseases. Pac. Symp. Biocomput. *25*, 463–474.

50. Morselli Gysi, D., do Valle, Í., Zitnik, M., Ameli, A., Gan, X., Varol, O., Ghiassian, S.D., Patten, J.J., Davey, R.A., Loscalzo, J., and Barabási, A.L. (2021). Network medicine framework for identifying drug-repurposing opportunities for COVID-19. Proc. Natl. Acad. Sci. USA *118*. e2025581118. https://doi.org/10.1073/pnas.2025581118.

51. Sügis, E., Dauvillier, J., Leontjeva, A., Adler, P., Hindie, V., Moncion, T., Collura, V., Daudin, R., Loe-Mie, Y., Herault, Y., et al. (2019). HENA, heterogeneous network-based data set for Alzheimer's disease. Sci. Data *6*, 151.

52. Kabir, M.T., Uddin, M.S., Mamun, A.A., Jeandet, P., Aleya, L., Mansouri, R.A., Ashraf, G.M., Mathew, B., Bin-Jumah, M.N., and Abdel-Daim, M.M. (2020). Combination drug therapy for the management of Alzheimer's disease. Int. J. Mol. Sci. *21*, 3272. https://doi.org/10.3390/ijms21093272.

53. Szklarczyk, D., Morris, J.H., Cook, H., Kuhn, M., Wyder, S., Simonovic, M., Santos, A., Doncheva, N.T., Roth, A., Bork, P., et al. (2017). The STRING database in 2017: quality-controlled protein–protein association networks, made broadly accessible. Nucleic Acids Res. *45*, D362–D368.

54. Davis, A.P., Murphy, C.G., Saraceni-Richards, C.A., Rosenstein, M.C., Wiegers, T.C., and Mattingly, C.J. (2009). Comparative Toxicogenomics Database: a knowledgebase and discovery tool for chemical-gene-disease networks. Nucleic Acids Res. *37*, D786–D792.

55. Davis, A.P., Grondin, C.J., Johnson, R.J., Sciaky, D., King, B.L., McMorran, R., Wiegers, J., Wiegers, T.C., and Mattingly, C.J. (2017). The comparative Toxicogenomics database: update 2017. Nucleic Acids Res. *45*, D972–D978.

56. Agora. https://agora.ampadportal.org/genes.

57. Carhart, R.E., Smith, D.H., and Venkataraghavan, R. (1985). Atom pairs as molecular features in structure-activity studies: definition and applications. J. Chem. Inf. Comput. Sci. *25*, 64–73. https://doi.org/10.1021/ci00046a002.

58. Durant, J.L., Leland, B.A., Henry, D.R., and Nourse, J.G. (2002). Reoptimization of MDL keys for use in drug discovery. J. Chem. Inf. Comput. Sci. *42*, 1273–1280.

59. Morgan, H.L. (1965). The generation of a unique machine description for chemical structures-A technique developed at chemical abstracts service. J. Chem. Doc. *5*, 107–113. https://doi.org/10.1021/c160017a018.

60. Nilakantan, R., Bauman, N., Dixon, J.S., and Venkataraghavan, R. (1987). Topological torsion: a new molecular descriptor for SAR applications. Comparison with other descriptors. J. Chem. Inf. Comput. Sci. *27*, 82–85. https://doi.org/10.1021/ci00054a008.

61. Landrum, G.. RDKit. https://www.rdkit.org/.

62. Fabregat, A., Jupe, S., Matthews, L., Sidiropoulos, K., Gillespie, M., Garapati, P., Haw, R., Jassal, B., Korninger, F., May, B., et al. (2018). The reactome pathway knowledgebase. Nucleic Acids Res. *46*, D649–D655.

63. Kanehisa, M., Furumichi, M., Tanabe, M., Sato, Y., and Morishima, K. (2017). KEGG: new perspectives on genomes, pathways, diseases and drugs. Nucleic Acids Res. *45*, D353–D361.

64. Subramanian, A., Tamayo, P., Mootha, V.K., Mukherjee, S., Ebert, B.L., Gillette, M.A., Paulovich, A., Pomeroy, S.L., Golub, T.R., Lander, E.S., and Mesirov, J.P. (2005). Gene set enrichment analysis: a knowledge-based approach for interpreting genome-wide expression profiles. Proc. Natl. Acad. Sci. USA *102*, 15545–15550.

65. Hamilton, W.L., Ying, R., and Leskovec, J. (2017). Inductive Representation Learning on Large Graphs.

66. Gaudelet, T., Day, B., Jamasb, A.R., Soman, J., Regep, C., Liu, G., Hayter, J.B.R., Vickers, R., Roberts, C., Tang, J., et al. (2021). Utilizing graph machine learning within drug discovery and development. Brief. Bioinform. https://doi.org/10.1093/bib/bbab159.

67. Percha, B., and Altman, R.B. (2018). A global network of biomedical relationships derived from text. Bioinformatics *34*, 2614–2624.

68. Law, V., Knox, C., Djoumbou, Y., Jewison, T., Guo, A.C., Liu, Y., Maciejewski, A., Arndt, D., Wilson, M., Neveu, V., et al. (2014). DrugBank 4.0: shedding new light on drug metabolism. Nucleic Acids Res. *42*, D1091–D1097.

69. Himmelstein, D.S., Lizee, A., Hessler, C., Brueggeman, L., Chen, S.L., Hadley, D., Green, A., Khankhanian, P., and Baranzini, S.E. (2017). Systematic integration of biomedical knowledge prioritizes drugs for repurposing. Elife *6*, e26726. https://doi.org/10.7554/elife.26726.

70. Szklarczyk, D., Gable, A.L., Lyon, D., Junge, A., Wyder, S., Huerta-Cepas, J.,

Simonovic, M., Doncheva, N.T., Morris, J.H., Bork, P., et al. (2019). STRING v11: protein–protein association networks with increased coverage, supporting functional discovery in genome-wide experimental datasets. Nucleic Acids Res. *47*, D607–D613.

71. IntAct IntAct. https://www.ebi.ac.uk/intact/.

72. Fey, M., and Lenssen, J.E. (2019). Fast Graph Representation Learning with PyTorch Geometric.

73. Yu, T., Kumar, S., Gupta, A., Levine, S., Hausman, K., and Finn, C. (2020). Gradient Surgery for Multi-Task Learning.

74. Oset-Gasque, M.J., and Marco-Contelles, J. (2018). Alzheimer's disease, the "one-molecule, one-target" paradigm, and the multitarget directed ligand approach. ACS Chem. Neurosci. *9*, 401–403. https://doi.org/10.1021/acschemneuro.8b00069.

75. Ling, Y., Upadhyaya, P., Chen, L., Jiang, X., and Kim, Y. (2021). Heterogeneous Treatment Effect Estimation Using Machine Learning for Healthcare Application: Tutorial and Benchmark.

76. Hernán, M.A., and Robins, J.M. (2016). Using big data to emulate a target trial when a randomized trial is not available. Am. J. Epidemiol. *183*, 758–764.

77. Pearl, J. (2000). Causality: Models, Reasoning, and Inference (Cambridge University Press).

78. Pearl, J. (2014). Probabilistic Reasoning in Intelligent Systems: Networks of Plausible Inference (Elsevier).

79. Kim, Y., Kim, K., Park, C., and Yu, H. (2019). Sequential and diverse recommendation with long tail. In Proceedings of the Twenty-Eighth International Joint Conference on Artificial Intelligence. https://doi.org/10.24963/ijcai.2019/380.

80. Rendle, S., Freudenthaler, C., Gantner, Z., and Schmidt-Thieme, L. (2012). BPR: Bayesian Personalized Ranking from Implicit Feedback.

STAR★METHODS

KEY RESOURCES TABLE

REAGENT or RESOURCE	SOURCE	IDENTIFIER
Software and algorithms		
Python	https://www.python.org/	RRID:SCR_008394
Pytorch-geometrics	https://www.pyg.org/	–
Deposited data		
Comparative Toxicogenomics Database	http://ctdbase.org/	RRID:SCR_006530
STRING	https://string-db.org/cgi/download?sessionId=bVNgzWswuCA8	RRID:SCR_005223
ClinicalTrials.gov	http://clinicaltrials.gov/	RRID:SCR_002309
Alzforum	http://www.alzforum.org/	RRID:SCR_006416
Alzped	https://alzped.nia.nih.gov	RRID:SCR_021230
Agora	https://agora.adknowledgeportal.org/	–
Experimental models: Cell lines		
HT22	https://web.expasy.org/cellosaurus/CVCL_0321	RRID:CVCL_0321

RESOURCE AVAILABILITY

Lead contact

Further information and requests for resources and reagents should be directed to and will be fulfilled by the lead contact, Yejin Kim (Yejin.Kim@uth.tmc.edu).

Materials availability

This study did not generate any new reagents.

Data and code availability

- All interaction data used in this study are publicly available from CTD, STRING, Agora, ClinicalTrial.gov, and AlzPED.
- Experimental results are available in supplemental information.
- All original code has been deposited at https://github.com/freshnemo/AD-KG, and is publicly available as of the date of publication.

METHOD DETAILS

Build Alzheimer's disease knowledge graph

To construct a high-quality Alzheimer's Disease (AD) knowledge graph that represents the disease-related biological interactome, we extracted and harmonized three major data sources that contain the following interaction types: (1) Universal protein-protein interactions from STRING;[53] (2) Interactions between genes, drugs, GO, and pathways from the Comparative Toxicogenomics Database (CTD);[54,55] (3) Drug-drug associations based on four types of structural similarity fingerprints. Genes were annotated to their Entrez IDs assigned by the National Center for Biotechnology Information (NCBI) database. Details of each relation type will be described later in discussion.

Drugs and genes

We collected precompiled drug-gene interactions from CTD, including 6,543 unique FDA-approved drugs or experimental compounds, as well as 16,997 genes that interact with those drugs. 119 drugs have direct

evidence reporting either the drugs' relevance to AD etiology (e.g., Streptozocin) or treatment (e.g., Donepezil). The remaining drugs are from literature reporting the potential efficacy of the drugs. 117 genes have direct evidence reporting either the gene's relevance to AD etiology (e.g., APOE) or treatment (e.g., LEP). The remaining genes are from literature reporting the potential relevance of the genes to AD. The 110,637 drug and target gene interactions are from literature with cell-based or animal-based evidence.

Gene and gene

We retrieved gene-gene interaction from the STRING database, which collected seven types of evidence for protein-protein interaction: biological experiment, pathway inference, text mining, gene co-expression, neighborhood genes in chromosomes, fusion, and co-occurrence.[53] We selected 123,738 protein-protein interactions that have >95% combined confidence scores across the seven points of evidence.

AD-related genes

To highlight important genes related to disease progression or treatment strategies in the AD knowledge graph, we extracted high-confident AD-related genes from (1) Agora's nominated gene list, identified and validated by researchers from the National Institute on Aging's Accelerating Medicines Partnership in Alzheimer's Disease (AMP-AD) consortium;[56] (2) CTD's gene list, with direct evidence of being a biomarker or a therapeutic target. In total, we obtained 743 AD-related genes, which were utilized in the node classification task (see Method 4).

Drug and drug structural similarity

A drug with a similar structure usually accompanies similar targets. To best represent each compound's chemical structure, we utilized four types of fingerprints: atom-pair fingerprints,[57] MACCS fingerprint,[58] Morgan/Circular,[59] and Topological-torsion fingerprints.[60] Sørensen–Dice similarity coefficients were computed between every two drugs (or compounds) using RDkit (version 2021.03.4).[61] For each type of fingerprint, we calculated the *Z score* of the Sørensen–Dice coefficient to obtain pairwise compound similarity and defined compound pairs with *Z score*>=3 to be structurally similar. In total, we determined 37,669 compound pairs that are structurally similar to each other.

Pathway and AD-related genes

For each AD-related gene, CTD linked them with their involved pathways from Reactome[62] and KEGG[63] databases. Various pathways of a multifactorial disease such as AD can display the diverse etiology and mechanisms of the disease. Querying "Alzheimer's Disease" from CTD, we extracted 1,778 gene-pathway interactions containing 678 unique pathways.

Pathway and drugs

Among 6,543 drugs of interest, their drug targets from CTD were used to query related Reactome[62] and KEGG[63] pathways and computed enriched drug-pathway associations using Enrichr.[64] For each drug, enriched pathways for all its target genes were identified using a threshold of p value <0.05. Drugs and their enriched pathways were connected as drug-pathway interactions. There are 110,637 drug-pathway interactions, including 1,622 pathways in our knowledge graph.

GO and AD-related genes

Gene ontologies are structured and controlled vocabularies that represent each gene's participating biological processes, molecular functions, and cellular components. We extracted gene ontologies for AD-related genes from CTD to construct gene-GO edges. A total of 7,368 gene-GO interactions were collected between 89 AD risk genes and 2,965 unique GO terms.

GO and drugs

CTD also inferred associations between GO and certain drugs under Alzheimer's Disease. Drug-GO interactions were established based on either a combination of curated drug-GO interactions and drug-AD interactions, or a gene-GO annotation in AD or both. These expanded our AD knowledge graph with 6,817 drug-GO interactions, including 2,377 unique GO terms and 108 unique drugs.

Knowledge graph representation

Graph neural network (GNN) is one field of deep neural networks that derive a vectorized representation of nodes, edges, or whole graphs. Adopting GNN into the biomedical network facilitates the integration of multimodal and complex relationships. The graph node embedding can preserve the node's local role and global position in the graph via iterative and nonlinear message passing and aggregation. It learns the structural properties of the neighborhood and the graph's overall topological structure,[65] thus allowing us not only to restore the known interactions but also infer unknown interactions. The knowledge graph representation that contains such putative interactions can help us find new indications of drugs.[66] Recently GNN has demonstrated a great advance in predicting hidden interactions (e.g., PPIs, drug-drug adverse interactions, and drug-target interactions) and the discovery of new molecules.[23,24] GNN is also used to derive representation from a graph with multiple types of relations and nodes (i.e., heterogeneous network or knowledge graph). The Drug Repurposing Knowledge Graph (DRKG)[18] uses the knowledge graph representation to capture whole topological relations from seven biomedical databases.[18,67] The knowledge graph includes 97,238 nodes (from 13 node types including gene, molecular function, pathway, disease, symptom, anatomy, cellular component, compounds, side effect, ATC, and pharmacologic class) and 5,874,261 interactions (from 107 edge types) from DrugBank,[68] HetioNet,[69] GNBR,[67] STRING[70] and IntAct.[71] Their representation offers a general and universal embedding of these entities, which can further enrich other domain-specific knowledge representations.

In this study, we developed the knowledge graph representation model by customizing the deep variational graph neural autoencoders (VGAE) to incorporate multiple types of relations or edges (Figure 1B).[19] The self-supervised graph autoencoder method encodes the nodes into a latent vector (embedding) and reconstructs the given graph structure (i.e., graph adjacency matrix) with the encoded latent vector. The variational graph approach can encapsulate the complex network into a probabilistic distribution (rather than deterministic vector representation) for nodes considering the uncertainties of our knowledge for AD; therefore, it alleviates the overfitting/underfitting issues due to partial knowledge. We customized the VGAE to incorporate the different types of edge by setting different weight matrices for each type of edge. This multi-relational approach respects the different propagation for each interaction type. Since our objective is to derive node embedding that reflects the overall graph topology, the multi-relational VGAE model was trained to reconstruct the missing interaction using the node embeddings as an autoencoding manner. For the optimization, in the message-passing step, each node (entity)'s embedding is iteratively updated by aggregating the neighbors' embedding, in which the aggregation function is a mean of the neighbor's features, concatenation with current embedding, and a single layer of a neural network on the concatenated one. PyTorch Geometric was used for model implementation.[72] The model structure was (1 × 400) → Graph convolution to (1 × 256) → RELU → Dropout → Summation of multiple edge types → Batch norm → Graph convolution to 1 × 128 (mean) and 1 × 128 (variance). We randomly split the knowledge graph edge (i.e., positive edges) into 90% for training and 10% for testing, and generated the same number of negative edges from which the positive edges will be predicted.

Transfer learning from a comprehensive drug knowledge graph

We boosted the node embedding's biological relevance in the AD knowledge graph with millions of interactions from public biomedical literature by transfer learning. Transfer learning is to transfer knowledge from previously learned universal models to domain-specific models. By transferring and fine-tuning the universal knowledge, the AD network embedding can respect universal pharmacological interactions while prioritizing AD-related interactions. Injecting this universal knowledge into the AD domain is critically important in addressing the uncertainty in AD knowledge. To achieve this task, we extracted the DRKG network,[18] which contains the universal embedding of 15 million pharmacological entities across 39 different types of interactions among genes and compounds from large biomedical databases including DrugBank, HetioNet, GNBR, STRING, IntAct, and DGLdb.[48] We avoided directly incorporating the edges of the DRKG network in our AD knowledge graph since the DRKG is comprehensive in breadth but shallow in depth. DRKG's network contains less accurate interactions (e.g., the same drug encoded in different drug nodes due to ID mismatching) that can be diluted into our small but specific AD knowledge graph.

Pretrained embedding for drugs, genes, pathways, and functional ontology were retrieved from DRKG and used as initial node features in our model, and fine-tuned them to the AD knowledge graph. When nodes in the knowledge graph were not matched to entities in the universal embedding, we learned the embedding as parameters (e.g., one hot to embedding vectors).

Node classification to differentiate AD-related genes in the knowledge graph

To leverage auxiliary information on known AD-related high-risk genes, we added a node classification task in our graph neural network model to differentiate the 743 AD-related genes (from Method 1) from the rest of genes in the graph. We hypothesized that one can predict AD-related genes using gene interaction with other genes, GO, and pathways, and the node classification task was to predict whether a gene is one of the AD-related genes using the gene representation in the AD knowledge graph. The node classification consists of two graph convolution layers (GraphSAGE) that sample a node's adjacent neighborhoods and aggregate their representation. The dimensions of those two convolution layers were Graph convolution (128, 64) → RELU → Dropout → Graph convolution (64, 1). We split the gene nodes into 90% for training and 10% for testing. As the labels are not balanced (only 743 AD-related genes out of 16,997 genes), we randomly split the gene nodes into 90% for training and 10% for testing while maintaining the ratio of AD gene and non-AD gene. This AD-related gene classification task was jointly optimized with the relational VGAE so that the AD knowledge graph representation can distinguish AD-related genes from all other genes. We used PcGrad,[73] a multi-task optimization technique that resolves conflict among multiple tasks' gradients by normal vector projections, to achieve a better local optimum.

Validating the quality of knowledge graph representation

We evaluated the quality of AD knowledge graph representation by checking whether the learned node embedding can restore the known edges. The edge prediction task is to predict whether an edge exists between head and tail nodes using the two nodes' embeddings. The edge prediction task's accuracy will be high if the node embedding encapsulates the edge information faithfully. For evaluation, we randomly set aside 10% of the edges for each edge type (Table S1). We sampled negative (or fake) but plausible edges at 1:5 ratio that do not exist in the knowledge graph by replacing tail nodes with other random nodes within the same node types and predicted whether a given edge is real or fake.[19] The model was trained using all edge types and evaluated separately for each edge type. We also ablated one edge type and observed how one edge type contributed to predicting all the edge types (Table S1). This experiment allowed us to determine which interactomes are unique and hard to be replaced or implicitly inferred by other edge types. The edge prediction accuracy was measured as general accuracy measure – the area under the receiver operating curve (AUROC) and the area under the precision-recall curve (AUPRC) and ranking accuracy measure – mean reciprocal rank (MRR), mean average precision (MAP), and precision at top *k*., considering the imbalance of positive and negative samples. For the node classification task to distinguish between AD-related genes and remaining genes, we also measured the classification accuracy using the AUROC and AUPRC.

Identification of multi-level evidence for drug efficacy

Next, we prioritized 6,543 drug candidates that are similar to drugs with historical evidence. AD is a complex disease and its effective therapeutic targets are largely unknown, thus drugs interacting with a few targets can have limited efficacy.[74] Holistic evidence may alternatively capture the efficacy in systemic and complex diseases. We believe the most desirable drug candidates would have multiple levels of complementary evidence to support their efficacy, such as post-treatment transcriptomic patterns, mechanistic efficacy in preclinical animal models, and epidemiological treatment effects in real-world patient data. We identified each evidence as follow:

Transcriptomic reversed patterns

We examined reversed patterns of the AD model's genetic signature and drug-induced gene signature using gene set enrichment analysis. We leveraged a recent study[9] and identified 149 drugs with significant transcriptomic reversed patterns. Among the 149 drugs, 76 drugs were matched to our 6,543 drug candidates.

Mechanistic efficacy in preclinical models

Alzheimer's Disease Preclinical Efficacy Database (AlzPED) accumulated preclinical evidence for effective AD drugs. We identified 338 drugs with significant efficacy from 791 animal-based studies targeting various pathologies including amyloid-beta, tau, and neuroinflammation. Among the 338 drugs, 189 drugs were matched to our 6,543 drug candidates.

Population-based treatment effect

We estimated drugs' population-based treatment effect as rel-world evidence of drug efficacy. Healthcare claim data is a unique resource to investigate treatment effects of prescribed drugs on reducing AD onset risk during the preclinical stage of AD. We used Optum's de-identified Clinformatics Data Mart subscribed by UTHealth. This billing-purpose claim data is inherently noisy and sparse, thus requires careful data preparation (e.g., setting observation windows to exclude subjects who are not old enough to have AD onset, identifying AD onset via billing-purpose diagnosis and medication codes, grouping high-dimensional diagnosis codes into clinical comorbidities as confounding variables). We followed the data preparation process in our previous work[75] based on target trials.[76] We calculated the average treatment effect among treated (ATT) using inverse probability of treatment weighting (IPTW).[77,78] See details at Supplementary Method 1. We identified 126 drugs with positive treatment effects (i.e., ATT<0 to reduce AD onset). Among the 126 drugs, 101 drugs were matched to our 6,543 drug candidates.

Clinical trials terminated at phase II/III

Many drugs in the failed clinical trials passed several phases and showed non-trivial response rates (e.g., good response on certain sub-populations). We hypothesize individual drugs (focusing on different targets) from previously failed clinical trials respond differently on sub-populations, and therefore, cocktails of complementary drugs might cover a larger population. Also, because drug testing in clinical trials is partially efficacious in treating AD, a drug that is similar to these trial drugs (and their combinations) can have potential efficacy too. We collected 294 drugs from 2,675 interventional clinical trials for AD from ClinicalTrial.gov. Among the 294 drugs, 210 drugs were matched to our 6,543 drug candidates.

Prioritizing repurposable drugs with multiple evidence

After collecting multi-level evidence of drug efficacies from Method 6, we built a multi-task ranking model to prioritize drugs from AD knowledge graph representation. To build a ranking model that takes into account four categories of evidence simultaneously, we adapted a neural network model with a pairwise ranking loss for each evidence.[79,80] For each task, the positive samples to prioritize were the drugs with the positive evidence, while negative samples were the remaining drugs in the AD knowledge graph. A fifth task was added to predict whether a drug has any evidence or not (has evidence = 1; no evidence = 0). Again, we utilized PcGrad[73] to handle the gradient inconsistency in the multi-task optimization. The architecture was two fully connected layers (with the size of 128→128→5) with residual connection, nonlinear activation (ReLU), dropout, batch norm in the middle, and the optimization loss (four pairwise ranking losses). For evaluation, we validated the ranking model by evaluating whether the positive drugs (drugs fall into any category of evidence) are ranked high. We measured the accuracy of the drug ranking model using the AUROC and AUPRC of top *k* drugs with 50% training and 50% test cross-validation. We purposely set the portion of the training set lower because the four categories of drug evidence are not our sole "gold standard" to prioritize drugs.

Drug combination identification

To identify efficacious drug combinations from top-ranked drugs, we applied the Complementary Exposure Pattern[37] analysis, which hypothesized that "a drug combination is therapeutically effective only if the targets of the drugs both hit the disease module, but they target a separate neighborhood." We searched the drug combinations within the top-ranked drugs. We counted the number of genes in the AD module that a drug combination hits, where the drug combination's targets are disjoint.

In vitro validation on safety, tolerability, drug combinations

Neuronal culture

Hippocampal neurons (HT-22) were cultured in DMEM (Sigma-Aldrich #D6429) supplemented with 10% FBS, and 1X Antibiotic-Antimycotic (#30-004-CI, Corning). Neurons were subcultured every 3-4 days at approximately 75–80% of confluence and kept in a T-75 flask in a 5% CO2 incubator at 37°C. For bioassays, the neurons were detached with 0.25% trypsin-EDTA (Sigma-Aldrich #T3924), pelleted at 300g, and diluted in fresh DMEM. Cells were counted with LUNA-II automated cell counter (Logos) and seeded in 96-well plates at 5000 cells/well the day before. Morphology was monitored with an inverted optical microscope (Olympus CKX31).

Drug combinations

All the drugs were ACS grade or higher purity, prepared fresh immediately prior to use in the bioassays. Stock solutions of the drugs were prepared by dissolving in DMSO (Sigma-Aldrich #) at 50 mM. Each active

compound was then diluted with DMEM to 200, 100, 50, and 25 μM. As a control, we employed DMEM with DMSO.

Cytotoxicity and oxidative stress responses

Cell Counting Kit-8 (Dojindo, #CK04) was used to determine cell viability, proliferation, and cytotoxicity, measuring the absorbance of water-soluble tetrazolium salt (reduced WST-8) at 450 nm. Neurons were subcultured in 96-well plates and dosed with the active drugs diluted in DMEM, incubated at 37°C, and absorbance measured after 24, 48, and 72 h of treatment (SynergyLX multi-mode plate reader, Biotek). Each treatment was performed in triplicates. Oxidative stress responses of dosed neurons were determined with Fluorometric Intracellular ROS kit (Sigma-Aldrich #MAK142). Cells were subcultured into Costa-Assay (Corning #3904) clear flat bottom, tissue culture treated, black-coated 96-well plates. Neurons were dosed with active drugs (as described), incubated for 24, 48, or 72 h, and then fluorescence of intracellular ROS was determined following the protocol of the kit using DCFDA as a fluorogenic sensor (lex = 650/lem = 675nm) (SynergyLX multi-mode plate reader, Biotek). The same protocol was followed using 10 μM $A\beta_{42}$ (Anaspec, #AS24224) in combination with active drugs at 50 μM to quantify intracellular ROS in neurons. Each treatment was performed in triplicates.

Imaging

Neurons were analyzed in fluorescence, bright-field, phase contrast, live-cell, and z stack imaging with Digital Imaging System Celena-S (Logos). Micrographs were analyzed with Fiji-Image J.

QUANTIFICATION AND STATISTICAL ANALYSIS

Data acquired from bioassays were normalized to control for each dataset, the normalized average is presented as mean ± SEM. SigmaPlot was used for the analysis.